Inorg. Chem. **2002**, *41*, 3457–3462

Polyatomic Clusters of the Triel Elements. Palladium-Centered Clusters of Thallium in $A_8Tl_{11}Pd$, A = Cs, Rb, K

Stefan Kaskel, Michael T. Klem, and John D. Corbett*

Ames Laboratory[1] and Department of Chemistry, Iowa State University, Ames, Iowa 50011

Received January 28, 2002

Reactions of the elements within welded Ta containers at ~600 °C followed by slow cooling give new $A_8Tl_{11}Pd_x$ products from an apparently continuous encapsulation of Pd atoms into the pentacapped trigonal prismatic anions in the isotypic rhombohedral ($R\bar{3}c$) A_8Tl_{11} phases. All systems also produce other phases at $x < 1$ as well, the simplest being the cesium system in which only trigonal $Pd_{13}Tl_9$ is also formed. $Cs_8Tl_{11}Pd_{0.84(1)}$ was characterized by single-crystal means as close to the upper x limit in that system ($R\bar{3}c$, $Z = 6$, $a = 10.6l0(1)$ Å, $c = 54.683(8)$ Å). The Pd insertion causes an expansion of the D_3 host anion, particularly about the waist, to generate a trigonal bipyramidal $PdTl_5$ unit (d(Pd–Tl) ~ 2.6–2.8 A) centered within a somewhat larger Tl_6 trigonal prism, the remainder of the Tl_{11} cluster. Strong Tl cage bonding is retained. Extended Hückel calculations show significant involvement of all Tl 6s, 6p and Pd 4d, 5s, 5p orbital sets in the central and cage bonding. The last valence electron is considered to be delocalized in a conduction band, as in A_8Tr_{11} examples, rather than occupying an antibonding e″ LUMO across a gap of ~2.4 eV.

Introduction

The triel (Tr) elements Ga, In, and Tl prove to be unique sources of numerous novel polyatomic networks or polyanions when one or the other is reacted with an alkali metal Na−Cs.[2,3] For a given triel, the amount and size of the alkali metal reducing agent appears to be the simplest variable that governs the size and morphology of the product. Limited amounts of the cation-former and, to some degree, the larger sized cations produce more network structures, whereas these products are often depolymerized, ultimately into discrete polyanions, by more and, to some degree, smaller reducing agents.[4] The monoanions maybe as small as the tetrahedra, Tr_4^{8-} formally, but so far only with sodium. (The less familiar, linear Tr_3^{7-} also occurs to a limited degree and under less clear circumstances.[5]) Monoanions as large as Tl_{13}, a centered icosahedron, are known at the other extreme.[6] In addition, tight associations of the cations with specific sites on the polyanions appear to be general and particularly important in product configurations and stabilities.[2,7] Some clusters turn out to be new examples of what were first described for the deltahedral polyboranes as closed-shell examples with electron-deficient delocalized bonding, the earliest empirical descriptions of their electronic requirements being via Wade's rules.[8] But the triels also furnish many more hypoelectronic cluster examples that are bonded with fewer electrons. The frequency and evidently the stability of such isolated "naked" clusters in general increase from gallium to thallium, whereas networks are more favored with gallium. These changes qualitatively appear to be responses to simple trends in the ionization energies and the $ns-np$ valence level separations.[2]

Accordingly, a greater number of more remarkable or irregular cluster members have been found with thallium. The larger homoatomic examples include Tl_6^{6-} ($\sim D_{4h}$),[9,10] Tl_7^{7-} ($\sim D_{5h}$),[11] Tl_9^{9-} ($\sim C_{2v}$),[12] and Tr_{11}^{7-} ($\sim D_{3h}$),[13−16] and

* Author to whom correspondence should be addressed. E-mail: jdc@ameslab.gov.

(1) This research was supported by the Office of the Basic Energy Sciences, Materials Sciences Division, U.S. Department of Energy (DOE). The Ames Laboratory is operated for DOE by Iowa State University under Contract No. W-7405-Eng-82.

(2) Corbett, J. D. *Angew. Chem., Int. Ed.* **2000**, *39*, 670.
(3) Belin, C.; Tillard-Charbonnel, M. *Prog. Solid State Chem.* **1993**, *22*, 59.
(4) Kaskel, S.; Corbett, J. D. *Inorg. Chem.* **2000**, *39*, 3086.
(5) Dong, Z.-C.; Corbett, J. D. *Inorg. Chem.* **1996**, *35*, 3107.
(6) Dong, Z.-C.; Corbett, J. D. *J. Am. Chem. Soc.* **1995**, *117*, 6447.
(7) Corbett, J. D. Abstracts of Papers, 219th National Meeting of the American Chemical Society, San Francisco, CA, March 2000; American Chemical Society: Washington, DC, 2000; INORG 327.
(8) Wade, K. *Adv. Inorg. Chem. Radiochem.* **1976**, *18*, 1.
(9) Dong, Z.-C.; Corbett, J. D. *J. Am. Chem. Soc.* **1993**, *115*, 11299.
(10) Dong, Z.-C.; Corbett, J. D. *Inorg. Chem.* **1996**, *35*, 2301.
(11) Kaskel, S.; Corbett, J. D. *Inorg. Chem.* **2000**, *39*, 778.
(12) Huang, D.-P.; Dong, Z.-C.; Corbett, J. D. *Inorg. Chem.* **1998**, *37*, 5881.

10.1021/ic020078b CCC: $22.00
Published on Web 06/04/2002

to these can be added the centered icosahedral $Tl_{13}^{10-,11-}$.[6] Heteratomic, centered members are now also known for the related $Tl_{12}M^{12-}$, M = Mg, Zn−Hg,[17,18] for $Tl_{10}Zn^{8-}$ and $In_{10}Zn^{8-}$ ($\sim D_{4d}$),[19,20] and in the isoelectronic $Tr_{10}M^{10-}$ ($\sim C_{3v}$, M = Ni and, in part, Pd and Pt).[21−23] The Tr_{11}^{7-} clusters, easily described as pentacapped trigonal prisms, are the most remarkable in their electronic deficiency, $2n - 4$ skeletal electrons (in which n is the number of the polyhedral vertexes) vs a normal $2n + 2$ for classical closo deltahedra. Some of this unusual result originates because of symmetry.

We present here the first evidence of the remarkable direct insertion of a Pd atom into the center of the known Tr_{11}^{7-} cluster, namely, to give $Tl_{11}Pd^{7-}$. Both the atom and orbital sizes of the two components and the more stable anionic characteristics of thallium appear important in this presently singular process.

Experimental Section

Synthesis. The materials and general reaction techniques in welded tantalum tubes have been described elsewhere[4] except for the Pd source, which was from Alfa, −60 mesh, 99.5% metals basis. All transfer operations were performed in N_2- or He-filled gloveboxes. Samples of $A_8Tl_{11}Pd_x$, A = Cs, Rb, K, were generally prepared by the fusion of the elements in welded tantalum tubes followed by heat treatment.

$Cs_8Tl_{11}Pd$. Exploratory reactions in the Cs−Tl−Pd system with atom proportions near 8:10:2 were first run at about 600 °C followed by slow cooling to near room temperature. The Guinier powder patterns of the products showed CsTl, $Cs_{15}Tl_{27}$,[24] and what appeared to be a phase similar to rhombohedral Cs_8Tl_{11}.[15] However, careful comparison with the calculated pattern for the last showed significant differences: shifted lines in the low-angle region and the absence of the second strongest diffraction line. Diffractometer searches on single crystals of the new ternary phase verified the distinctions, especially an increase in $\vec{c}$ of nearly 1 Å. A structural solution showed that this and Cs_8Tl_{11} were isostructural except for a Pd atom that centered the Tl_{11}^{7-} cluster, but this site occupancy was clearly variable (as were the lattice dimensions) and less than complete. The remainder of the Pd added for the stoichiometries near $Cs_8Tl_{11}Pd$ was found to be partitioned into the known phase $Pd_{13}Tl_9$.[25]

Various synthetic procedures were then tested, including diverse starting compositions, annealing pressed pellets at various temperatures, fusion followed by quenching, slow cooling, etc. These coupled with structural refinements showed that the Pd content in the clusters could be varied appreciably, from zero for empty Cs_8Tl_{11} to ∼84(1)% achieved from a $Cs_8Tl_{11}Pd_{1.5}$ composition that had been slowly cooled (1.25 °C/h) from ∼600 °C. On the other hand, larger proportions of $Pd_{13}Tl_9$ needles were produced when the same compositions were heated to ∼1000 °C or cooled faster. The melting point of the new phase is around 500 °C (according to observations following reactions run under different conditions). A trace of CsTl was the only other phase ever seen by X-rays, except that golden tinges suggested that small amounts of free Cs were usually present in the products for the loaded stoichiometries $Cs_8Tl_{11}Pd_x$. The stoichiometry for the synthesis at the above composition may be written as $Cs_8Tl_{11}Pd_{1.5} \rightarrow 0.96Cs_8Tl_{11}Pd_{0.84} + 0.054Pd_{13}Tl_9 + 0.35Cs$.

This describes the usual route employed; we did not literally insert Pd into previously synthesized A_8Tl_{11} phases.

No indium analogues of these phases could be found, and Pt or Hg would not center this thallium cluster.

$K_8Tl_{11}Pd_y$ and $Rb_8Tl_{11}Pd_z$. These systems are analogous in containing centered $Tl_{11}Pd_x^{7-}$ anions, but additional unknown side products also appear for the $y, z \sim 1$ compositions studied, and their numbers increase for larger y, z. One X-ray structural refinement of the potassium product gave $x = 0.54$ (below), whereas intermediate lattice dimensions, between those for K and Cs, were measured for the corresponding product of a reaction with a loaded $Rb_9Tl_{11}Pd_{1.1}$ composition, $a = 10.301(2)$ Å, $c = 52.915(2)$ Å. Neither gold nor mercury would form a comparable product with K_8Tl_{11}. Reactions near a $Na_8Tl_{11}Pd$ composition gave instead the approximate pattern of cubic NaTl but with line splittings that indicated a lower symmetry and, presumably, Pd substitution or addition.

Crystallography. $Cs_8Tl_{11}Pd_x$. These investigations followed standard procedures, mounting the brown, sometimes triangular crystals from diverse reaction products into thin-walled capillaries and examining these first by Laue and, sometimes, by precession photographs. Diffraction data sets were collected at room temperature for several crystals with the aid of either AFC6R Rigaku or Bruker SMART CCD diffractometers and Mo Kα radiation, after which the data were reduced, averaged, etc. in the usual manner. Structural solutions were guided by the powder pattern evidence that the structure of this particular product is closely related to that of the known rhombohedral Cs_8Tl_{11}. The first structure was solved with the aid of CCD data in a monoclinic space group, but the program PLATON showed that the positions developed were completely consistent with those in the $R\bar{3}c$ group of Cs_8Tl_{11}[15] except that the new model had a Pd atom centered in the Tl_{11} framework as well (R1 = 0.074 for an assumed 100% Pd). Larger U_{33} values occurred for Pd and Tl2, both of which fall on the 3-fold axis along $\vec{c}$, consistent with a substantial dimensional increase of that parameter. A parallel fractional occupancy for Pd became evident during the isotropic refinement. Thereafter, products from a variety of reactions run under different conditions were studied, following both the lattice constants, which increase with Pd content, and the refined occupancy values for Pd obtained by refinement of single-crystal data for seven examples. Only data for the crystal with the highest (84%) Pd content will be detailed here.

With previous experiences, the refinement of the most Pd-rich structure in space group $R\bar{3}c$ from Rigaku data proceeded directly and smoothly. (The centricity seemed clear in all data reduction results, and no reduced Cs occupancy was ever evidenced.) Some pertinent data are given in Table 1. Absorption (582.3 cm^{-1}) was corrected with the aid of 10 ψ scans over a 2 Θ range of 13.6−31.3°. The Pd occupancy refined to 84(1)% after an isotropic refinement of the whole structure had converged, varying both the Pd occupancy and its thermal parameter along with all other variables. Anisotropic refinement thereafter proceeded to conver-

(13) Sevov, S. C.; Corbett, J. D. *Inorg. Chem.* **1991**, *30*, 4875.
(14) Blase, W.; Cordier, G.; Somer, M. *Z. Kristallogr.* **1991**, *194*, 150.
(15) Dong, Z.-C.; Corbett, J. D. *J. Cluster Sci.* **1995**, *6*, 187.
(16) Henning, R. W.; Corbett, J. D. *Inorg. Chem.* **1997**, *36*, 6045.
(17) Dong, Z.-C.; Corbett, J. D. *Angew. Chem., Int. Ed. Engl.* **1996**, *35*, 1006.
(18) Tillard-Charbonnel, M. M.; Belin, C. H. E.; Monteghetti, A. P.; Flot, D. M. *Inorg. Chem.* **1996**, *35*, 2583.
(19) Sevov, S. C.; Corbett, J. D. *Inorg. Chem.* **1993**, *32*, 1059.
(20) Dong, Z.-C.; Henning, R. Corbett, J. D. *Inorg. Chem.* **1997**, *36*, 3559.
(21) Henning, R. W.; Corbett, J. D. *Inorg. Chem.* **1999**, *38*, 3883.
(22) Sevov, S. C.; Corbett, J. D. *J. Am. Chem. Soc.* **1993**, *115*, 9089.
(23) Dong, Z.-C.; Corbett, J. D. Unpublished research.
(24) Dong, Z.-C.; Corbett, J. D. *Inorg. Chem.* **1996**, *35*, 1444.
(25) (a) Bhan, S.; Gödecke, T.; Panday, P. K.; Schubert, K. *J. Less-Common Met.* **1968**, *16*, 415. (b) Panday, P. K.; Schubert, K. *J. Less-Common Met.* **1969**, *18*, 175.

Table 1. Some Data Collection and Refinement Parameters for $Cs_8Tl_{11}Pd_{0.84(1)}$

fw	3400
space group, Z	$R\bar{3}c$ (No. 167), 6
lattice const[a]	
a (Å)	10.610(1)
c (Å)	54.683(8)
V (Å^3)	5331(1)
d_{calcd}, g cm^{-3}	6.387
abs coeff (Mo Kα, mm^{-1})	58.23
residuals: R; R_w[b]	0.036; 0.039

[a] Guinier data with Si as internal standard, $\lambda = 1.540562$ Å, 23 °C. [b] $R = \sum||F_o| - |F_c||/\sum|F_o|$; $R_w = [\sum w(|F_o| - |F_c|)^2/\sum w(F_o)^2]^{1/2}$.

gence with the Pd occupancy fixed at 84% but with its U values varying, the latter coming out close to those for other atoms in the structure. The final residuals R and R_w were 3.6% and 3.9%. The largest residual, 2.89 e$^-$/Å^3, lay 0.99 Å inside the waist Tl1 atom, this site presumably reflecting the largest Tl displacement without centering by Pd. Radial elongation of the Tl1 ellipsoid was found in another structural solution with a lower Pd content, 77(2)%.

$K_8Tl_{11}Pd_x$. A larger fraction of the palladium is lost in this system in the form of unknown phases. A crystal of the target phase isolated from a synthesis with the stoichiometry $K_8Tl_{11}Pd$ was characterized structurally to have a Pd occupancy of 54(2)% (R1 = 0.063, wR2 = 0.134 for $I > 2\sigma(I)$ data and with only modest Fourier difference map peaks, ≤3.6 e$^-$/Å^3). (All data for this study are contained in the Supporting Information.) However, the waist Tl1 atoms showed 3:1 ellipsoids that were strongly directed outward whereas the ellipsoids on axial Tl2 had a 1.5-fold elongation along $\vec{c}$. These both follow the principal distortions of the parent structure on centering Pd (below) and are appropriate for about equal proportions of empty and filled cluster.

This disordered $R\bar{3}c$ model appeared to be the best but not a very satisfactory resolution of the structure of the potassium phase. No superstructure reflections could be found on precession photographs exposed for 1 week. These photographs and the Rigaku data set did show a few violations of the *c*-glide condition. The highest symmetry rhombohedral subgroup that would allow an ordered Pd structure is $R32$, for which half of the clusters could be empty. Refinement of this model yielded R1 = 0.064, wR2 = 0.135 for $I > 2\sigma(I)$ data. However, the Pd ellipsoid was elongated along $\vec{c}$ by a factor of 3, the waist Tl1 atoms likewise appeared strongly disordered, and the model was generally unsatisfactory. Further symmetry reduction to $R3$ resulted in large correlation coefficients between parameters of formerly equivalent atoms and a poor refinement. There also appeared to be violations of the R-centering, but the study was not carried further after precession photographs did not yield a clear space group assignment.

Calculations. MO and overlap population data for the $Tl_{11}Pd_{1.0}$ anion with the refined structural model were calculated utilizing CAESAR,[26] with the following atom parameters:[27] (H_{ii} (eV) and ζ) Tl 6s, −11.6, 2.3; 6p, −5.8, 1.6; Pd, 5s, −7.32, 2.19; 5p, −3.75, 2.152; 4d, −12.02, 5.98, 0.52644 (c1), 2.613, 0.63733 (c2).

Results and Discussion

Although free Pd can be readily encapsulated in the Tl_{11}^{7-} clusters already known in A_8Tl_{11} (A = K, Rb, Cs), the conversion is incomplete, and other phases are also formed. For reactions in the pseudobinary Cs_8Tl_{11}−Pd system, the uptake of Pd is accompanied only by the precipitation of some of the intermetallic phase $Pd_{13}Tl_9$ plus a corresponding remainder of excess Cs. It is also evident that the yields and Pd contents of the target phase depend appreciably not only on the loaded composition $Cs_8Tl_{11}Pd_x$ but also on the thermal history of the samples, the highest content being obtained after slow cooling from ∼600 °C. Under these circumstances, the $\vec{c}$ lattice dimension evidently increases smoothly with Pd added from that of the nominally isostructural Cs_8Tl_{11} up to that from a Pd:Cs_8Tl_{11} = 2.0:1 composition, as shown in Figure 1 for earlier reactions run under less than optimal conditions. (The changes in $\vec{a}$ are qualitatively similar.) However, the nature of the variations shown in Figure 1 cannot be readily understood unless $Pd_{13}Tl_9$ also exhibits a variable stoichiometry, inasmuch as another degree of freedom that would be afforded by yet another significant product is not found. (Only a single set of lattice constants for $Pd_{13}Tl_9$ was given in the 1968−1969 reports, but the phase diagram provided showed a phase breadth of ≈3.5 atom %, and some mixed site occupancies were also discussed.[25]) We established actual Pd contents via several single-crystal studies of products from the better syntheses, for which these occupancies varied from 68(4)% to 84(1)%. Only the structure of the phase with the highest Pd content found is detailed here. (The difference between *c* lattice constants for the data crystal and the apparent upper limit in Figure 1 and its Pd occupancy are probably within the reproducibility of the synthesis.) This upper limit for Pd in the cluster phase can be understood as that for which the Pd activity is equal to that in the Pd-richest composition of ∼$Pd_{13}Tl_9$ and the next phase, Pd_2Tl.

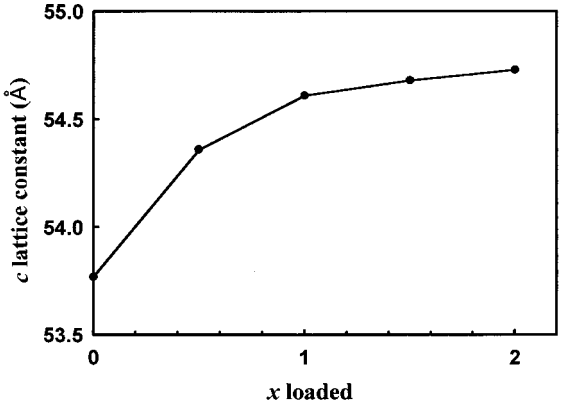

Figure 1. The course of the $\vec{c}$ lattice dimensions according to x in the loaded composition $Cs_8Tl_{11}Pd_x$ for samples slowly cooled from ∼700 °C.

Structural. The positional and distance data for $Cs_8Tl_{11}Pd_{0.84}$ are given in Tables 2 and 3. A view of the $Cs_8Tl_{11}Pd_{0.84}$ cluster is given in Figure 2 with 75% probability ellipsoids, the atom-numbering scheme, and some surface bond lengths. This figure also emphasizes that the pentacapped trigonal prismatic cluster is built of three independent Tl atom types, the lighter colored trigonal prismatic Tl3 atoms (6), the redder waist-capping Tl1 (3), and Tl2 axial caps (2). (The symmetry is D_3, but it is close to D_{3h} as the trigonal prismatic Tl3 atoms are nearly eclipsed.) In order to appreciate the sizable distortions that occur on Pd encapsulation, internal dimensions for empty clusters in Cs_8Tl_{11}[15] are shown at the top

(26) CAESAR: Ren, J.; Liang, W.; Whangbo, M.-H. PrimeColor Software, Inc.: Raleigh, NC, 1998.
(27) Alvarez, A. *Tables of Parameters for Extended Hückel Calculations*; Barcelona, Spain, 1987; Parts 1 and 2.

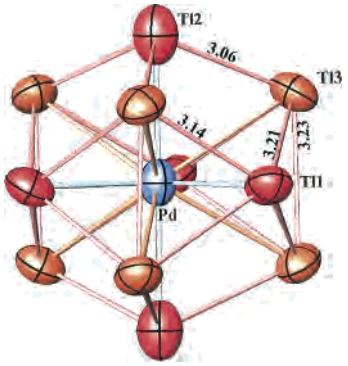

Figure 2. The $Tl_{11}Pd_{0.84}^{7-}$ cluster in $Cs_8Tl_{11}Pd_{0.84(1)}$, with anisotropic ellipsoids at the 75% probability level, the atom-numbering scheme, and some cage dimensions. The trigonal prismatic Tl3 atoms are somewhat more orange.

Table 2. Atomic Coordinates and Isotropic Equivalent Displacement Parameters ($Å^2 \times 10^3$) for $Cs_8Tl_{11}Pd_{0.84}$

atom	*x*	*y*	*z*	U_{iso}
Tl1	0.02464(3)	0	1/4	51.4(8)
Tl2	0	0	0.30109(6)	57.9(6)
Tl3	0.3972(2)	0.0694(2)	0.05378(3)	45.5(5)
Cs1	0.2873(3)	0.3688(4)	0.02118(4)	61.6(10)
Cs2	0	0	0.07842(8)	59.6(10)
Pd[a]	0	0	1/4	54.1(2)

[a] Occupancy = 0.84(1).

Table 3. Important Distances (Å) in $Cs_8Tl_{11}Pd_{0.84(1)}$

atoms	distance	atoms	distance
Tl1−Tl1	4.527(3)	Tl3−Tl3	4.902(3)
Tl1−Tl2	3.827(3)	Tl3−Cs1	3.995(3)
Tl1−Tl3	3.135(2)	Tl3−Cs1	4.117(3)
Tl1−Tl3	3.207(2)	Tl3−Cs1	4.281(3)
Tl1−Cs1	3.770(3)	Tl3−Cs2	4.125(2)
Tl1−Cs2	4.086(2)	Tl3−Cs2	4.401(2)
Tl1−Pd1	2.614(3)	Tl3−Pd	3.259(2)
Tl2−Tl3	3.065(2)	Cs1−Cs1	4.247(4)
Tl2−Cs1	4.150(3)	Cs1−Cs1	4.574(6)
Tl2−Cs1	4.269(3)	Cs1−Cs1	5.105(5)
Tl2−Pd	2.794(3)	Cs1−Cs2	4.705(4)
Tl3−Tl3	3.234(3)	Cs1−Cs2	4.740(4)

(a) of Figure 3 together with the related dimensions of the cluster refined with 84% Pd at the bottom (b). The former is clearly not very spherical, and the edges of the basal faces are over 5 Å.

Expansion of the cluster along Tl2−Tl2 on the 3-fold axis (vertical) and, especially, within the triangle of waist Tl1 atoms normal to this is necessary to achieve close and approximately equal Pd−Tl distances to these five atoms, changes that are also qualitatively reflected in the lattice dimension alterations. The ellipsoidal data (Figure 2) give no clear indication of the presence of ~16% empty clusters, but the largest residual (2.89 $e^-/Å^3$) is 1 Å inside Tl1. The disorder was more evident in structural studies of $K_8Tl_{11}Pd_{0.54}$ (Experimental Section, Supporting Information) which gave a less suitable description because the results clearly reflected a disordered mixture of centered and empty clusters in about equal proportions. We will return to the bonding within the cluster later.

Numerically, a 0.45 Å outward or radial displacement of the Tl1 waist atoms (equivalent to a 0.793 Å increase in *d*(Tl1···Tl1) is necessary to center Pd in Tl_{11}^{7-}, Figure 3b.

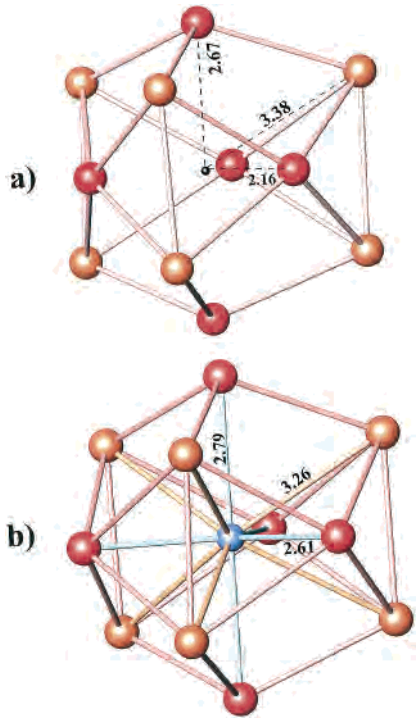

Figure 3. Internal dimensions of the cluster anions in (a) Cs_8Tl_{11} and (b) $Cs_8Tl_{11}Pd_{0.84}$. Note the sizable reapportionment of the cluster dimensions on Pd encapsulation.

There is also a smaller 0.24 Å increase in the overall axial length, *d*(Tl2−Tl2). These two changes also have the natural effect of lengthening the separation between the two types of capping atoms, Tl1−Tl2, by nearly 0.40 Å to 3.827 Å (overlap population = 0.09), well removing these from the range of "bonding" Tl−Tl distances found elsewhere in the cluster, 3.06−3.26 Å. The basal faces of the trigonal prism Tl3···Tl3 also contract by 0.24 Å (to 4.90 Å) on insertion of Pd. These last two changes appear necessary in order to maintain fairly constant Tl−Tl distances and bonding (below) around the distorted Tl_{11} skeleton, namely, to give changes of only +0.06 and +0.07 Å in the two independent *d*(Tl1−Tl3), −0.08 Å in *d*(Tl2−Tl3), and +0.01 Å in the length of the vertical trigonal prismatic edge, *d*(Tl3−Tl3). The end result of the added Pd bonding is a D_{3h} trigonal bipyramidal $PdTl_5$ group with Pd−Tl dimensions of 2.613(3) Å about the waist and 2.793(3) Å along the 3-fold axis, which dimension is commonly larger. Retention of reasonable Tl_{11} framework bonding elsewhere necessarily requires that the six remaining Pd−Tl3 distances to atoms defining the trigonal prism remain comparatively longer, 3.258 Å, a separation that is still 0.12 Å less than that to the center of the empty cluster.

The new $Tl_{11}Pd_{0.84}^{7-}$ is concluded to be isoelectronic with Tl_{11}^{7-} except for the added d^{10} core on Pd. The latter homoatomic thallium clusters are well established not only for the isostructural binary A_8Tl_{11}, A = K, Rb, Cs, but also for indium and gallium analogues. The entire family exhibits the unusual characteristic of a $R\bar{3}c$ lattice that contains eight cations even though it seems clear theoretically that all of the Tr_{11} anions are closed shell with a negative charge of

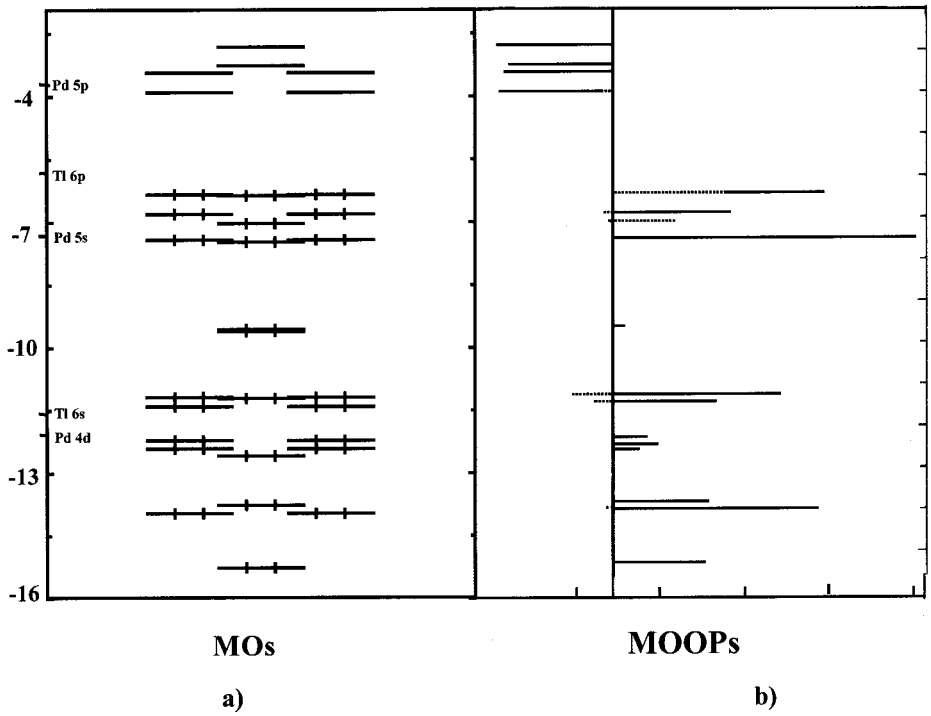

Figure 4. The extended Hückel results for $Tl_{11}Pd^{7-}$: (a) MO levels; (b) (molecular orbital) overlap populations, with Tl−Tl and Tl−Pd contributions superimposed as solid and dotted lines, respectively. The last electron is evidently delocalized in a conduction band and is not marked in panel a.

only seven.[13,15,28] In other words, addition of neutral Pd to an $(A^+)_8Tl_{11}^{7-}$ e^- salt with retention of the same $R\bar{3}c$ structure strongly implies that the ternary is also a metallic salt, as suggested by theory as well (below). This structure type is evidently more stable, and the Madelung energy in particular is greater, when one (or more) extra cation per formula unit is incorporated, the last electron evidently being delocalized in a conduction band. (Cs_8Ga_{11} is an exception to the last.[16]) Further support of the constitution $(A^+)_8Tl_{11}^{7-}$ e^- for the binary is the fact that nine examples of oxidized isotypic $A_8Tr_{11}X$ phases have also been synthesized for X = Cl, Br, I, and the measured $Cs_8Ga_{11}Cl$ member is diamagnetic.[16]

The novel $Tl_{11}Pd^{7-}$ represents the first case in which the empty analogue of a centered cluster is also known. Other stuffed triel clusters include potassium salts of the Zn-centered antiprismatic $In_{10}Zn^{8-}$ and $Tl_{10}Zn^{8-}$ (D_{4d})[19,20] and the isoelectronic $K_{10}Tr_{10}M$, Tr = In, Tl, M = Ni, Pd, Pt[22,23] plus $Na_{10}Ga_{10}Ni$.[21] The latter group of clusters have only $\sim C_{3v}$ symmetry (∼tetracapped trigonal prisms of In), which are thought to arise because of the need to accommodate 10 rather than eight cations in close association with the surfaces of each polyanion (below).

Bonding. The extended Hückel MO calculation results for the stoichiometric $Tl_{11}Pd$ cluster contain many of the features we expect from earlier studies on other centered examples of triel cluster anions. However, differences in the orbital sizes and energies generate some distinctive variations. The MOs are shown on the left in Figure 4 along with the (MO) overlap populations on the right; the Tl−Tl and Tl−Pd values in the latter are superimposed solid and dotted lines, respectively. The five 4d orbitals on Pd plus the 11 Tl 6s states are the principal components of the bottom 16 levels, up to −9.61 eV. The energy decrease for some of the latter is significant. Above these are the nine mainly Tl p-orbital-based states (−7.5 to −6.4 eV) that are occupied by 18 valence electrons, formally 11 from Tl 6p and 7 from the negative charge on the polyanion. Among the latter group are those that incorporate largely Pd 5s orbitals, and also appreciable Pd 5p contributions, and the largest Tl−Pd overlap populations come into play here. In terms of electron distributions and bond populations, the trigonal prismatic atoms provide the stronger overall glue and some reason for the stability of this arrangement as they bond to both the axial and waist atoms. Palladium bonds to waist and axial Tl atoms in about a 3:2 proportion according to the populations. Likewise the atom populations on waist, trigonal prismatic, and axial Tl correspond to charges of −0.36, −0.60, and −0.42 each, respectively, as could be qualitatively inferred from the number and lengths of the bonds about each. The corresponding formal (Mulliken) charge on palladium is −1.5. The average populations per Tl−Tl and Tl−Pd contacts are 0.52 and 0.16, respectively.

In some more detail, the 14 MOs up through −11.2 eV originate principally (but not exclusively) with Tl 6s. Thallium s−p hybridization appears in the MOs that fall between −11.4 and −9.6 eV, and Tl 6p affords the predominate bonding for thallium up to the effective HOMO at −6.4 eV. Involvement of Pd orbitals in the bonding is appreciable at nearly all levels. The Pd 4d set is predominantly split through mixing with Tl 5s states over the range of −11.2 to −12.6 eV (antibonding at the top; Figure 4b) although some Pd 4d is also found in the Tl p valence band around −6.8 eV. Palladium 5s is utilized in the MOs over a wide range, from one of the close pair of singlet levels near

(28) Llusar, R.; Beltrán, A.; Andres, J.; Silvi, B.; Savin, A. *J. Phys. Chem.* **1995**, *99*, 521.

−9.6 eV well into the empty antibonding states. The distinctive combination in this pair in the former (−9.65 eV) consists of Tl p_z π orbitals on the waist atoms combined with radial s−p hybrids on the trigonal prismatic and axial atoms, all on the cage, whereas the MO at −9.60 eV has a modest amount of Pd s combined with similar radial orbitals just for waist and prismatic atoms (a_1'). Note that both of these MOs have quite small overlap populations. In contrast, the lowest three MOs in the Tl p-band around −7.5 eV contain only Tl 6p, and negligible Tl 5s and Pd 5d. In contrast, the next (a_1', −7.1 eV) consists of radial hybrids on waist and axial Tl atoms combined with large amounts of Pd 5s and gives a significant Pd−Tl overlap population. Finally the last three MOs in the valence band involve significant Pd 5p bonding with Tl p, the antibonding counterparts lying much higher. The e″ LUMO above the 2.4 eV gap is, in contrast, antibonding (Figure 4b), largely π in character, and only on the cage. Thus we believe that the fifty-first electron, in parallel with all of the isotypic A_8Tr_{11} phases (except Cs_8Ga_{11}), is instead delocalized in the lattice so that the compound is metallic.

The distinctive differences in bonding between $In_{10}Ni^{10-}$ and $Tl_{11}Pd^{7-}$ appear to arise mainly from the markedly decreased bonding interactions of the smaller $3d^{10}$ core in nickel. The MOs for the $In_{10}Ni^{10-}$ cluster are similar in that the d^{10} states lie low, ∼5 eV below the valence states and ∼1 eV below In 5s, but the principal Ni−In bonding is only between Ni s and p and In p (and s).[22] An even more corelike $3d^{10}$ on Zn in $In_{10}Zn^{8-}$ is as expected.[19]

A general intimate and regular association of the cations with such polyanions has been noted before,[2,7] and this continues in $Cs_8Tl_{11}Pd_{0.84}$. Figure 5 shows the distinctive location of the 12 nearest cesium cations (green) about the $Tl_{11}Pd$ cluster. These sort out in a very regular manner into six 4-bonded Cs1 that cap the nearly planar quadrilateral faces (Tl1−Tl3−Tl2−Tl3), three above and three below in the figure, plus six Cs2 that each cap triangular faces around the cluster waist, namely, those formed by a vertical Tl3−Tl3 edge plus a Tl1 atom. The cation−anion packing seems relatively tight as the two shortest types of Cs1···Cs2 distances (Table 3) are found in this cation sheath. Furthermore, the shortest Cs1−Cs1 separation occurs within the next larger cation shell (not shown) in which six Cs1 atoms bridge all Tl2−Tl3 edges at the top and bottom of the cluster. It should be realized that the cations considered here have like or related bonding functions on neighboring clusters, as well, including still more distant exo contacts at the thallium vertexes.

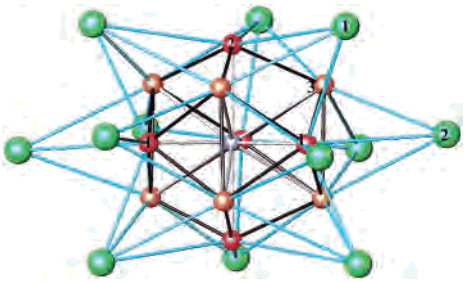

Figure 5. The two sets of nearest cesium cations about $Tl_{11}Pd^{7-}$ that separately cap six quadrilateral Tl1−Tl3−Tl2−Tl3 (Cs1) and six triangular Tl3−Tl3−Tl1 (Cs5) faces thereon.

Remarkable intermetallic cluster ions illustrated here by $Tl_{11}Pd^{7-}$ can scarcely be predicted, let alone imagined. Exploratory synthesis is accordingly the best and perhaps only practical way to uncover such novel solid state species. The new ion shows a quite new and novel configuration, a trigonal bypramidal $PdTl_5$ encased in a somewhat larger trigonal prism, both of which are easily derived from the parent Tl_{11}^{7-} by distortion. With present knowledge, the size and d, s, p orbital energies of Pd appear particularly suitable for the formation of $Tl_{11}Pd^{7-}$. There is little doubt that we have not seen the end of this sort of species.

Acknowledgment. S.K. was supported in part by a Feodor-Lynen Fellowship from the A. v. Humboldt Foundation, Bonn, Germany. We are indebted to Dong-Kyun Seo for assistance with some calculational problems.

Supporting Information Available: Tables containing data collection and anisotropic displacement parameters for the $R\bar{3}c$ structures of $Cs_8Tl_{11}Pd_{0.84}$ and $K_8Tl_{11}Pd_{0.54}$ plus atom positions for and distances within the latter. This material is available free of charge via the Internet at http://pubs.acs.org.

IC020078B